

Fig.1

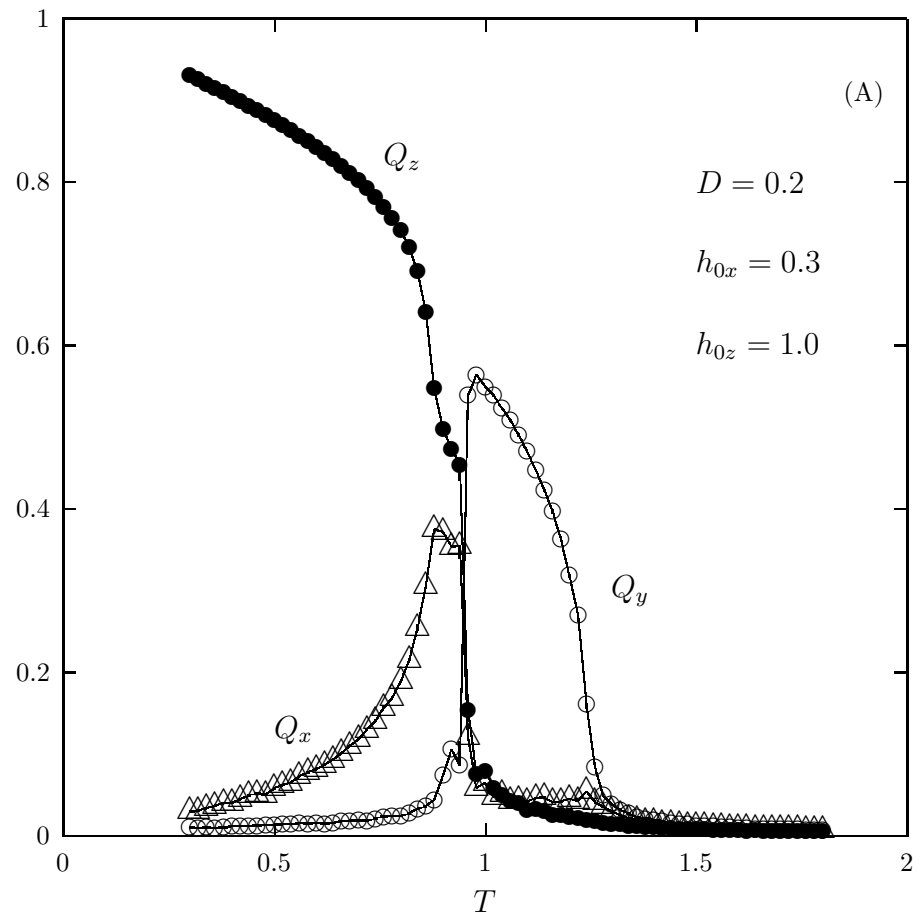


Fig.2a

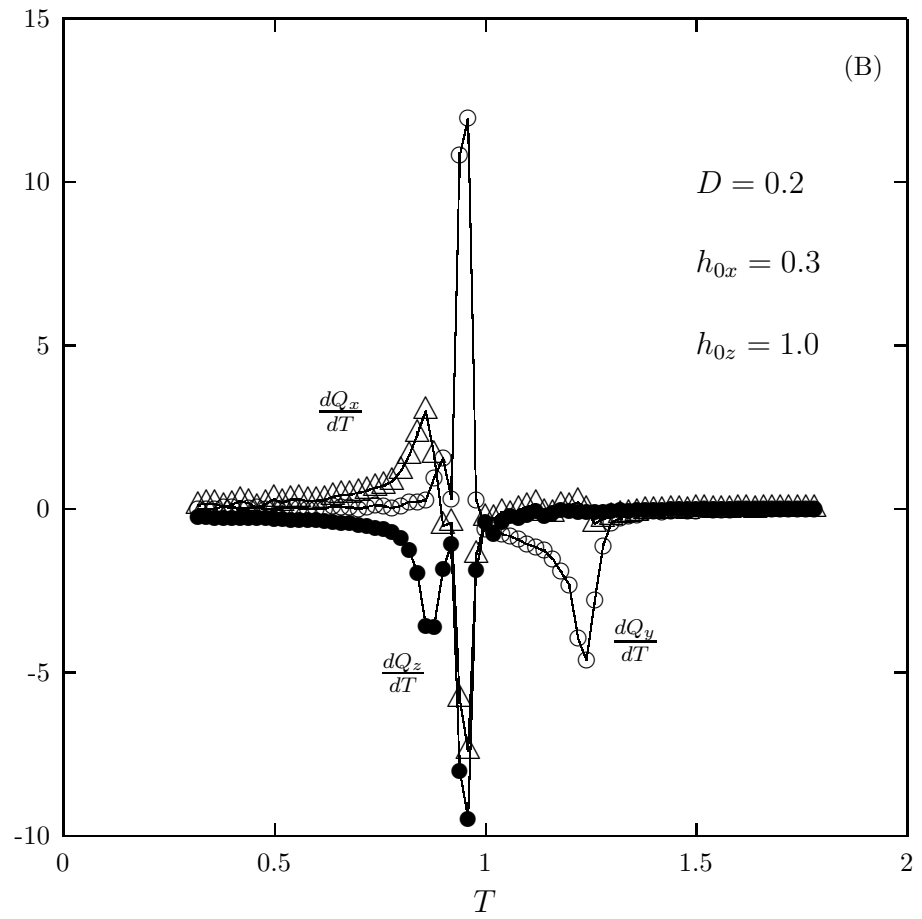


Fig.2b

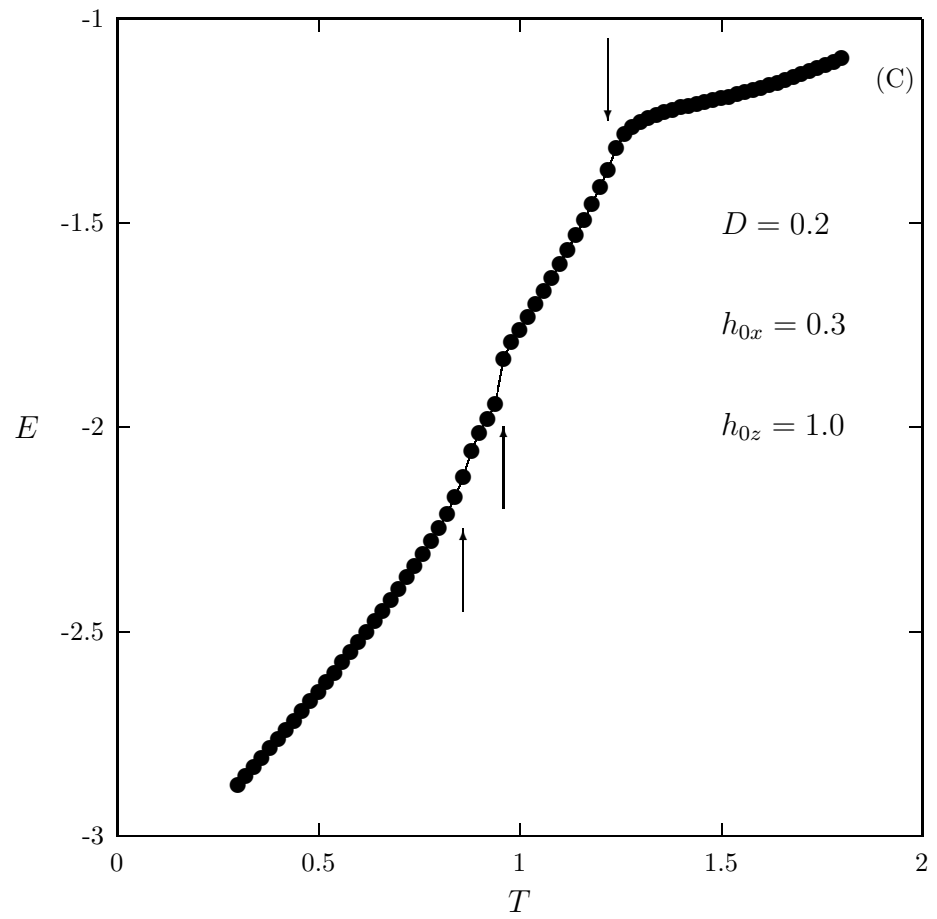


Fig.2c

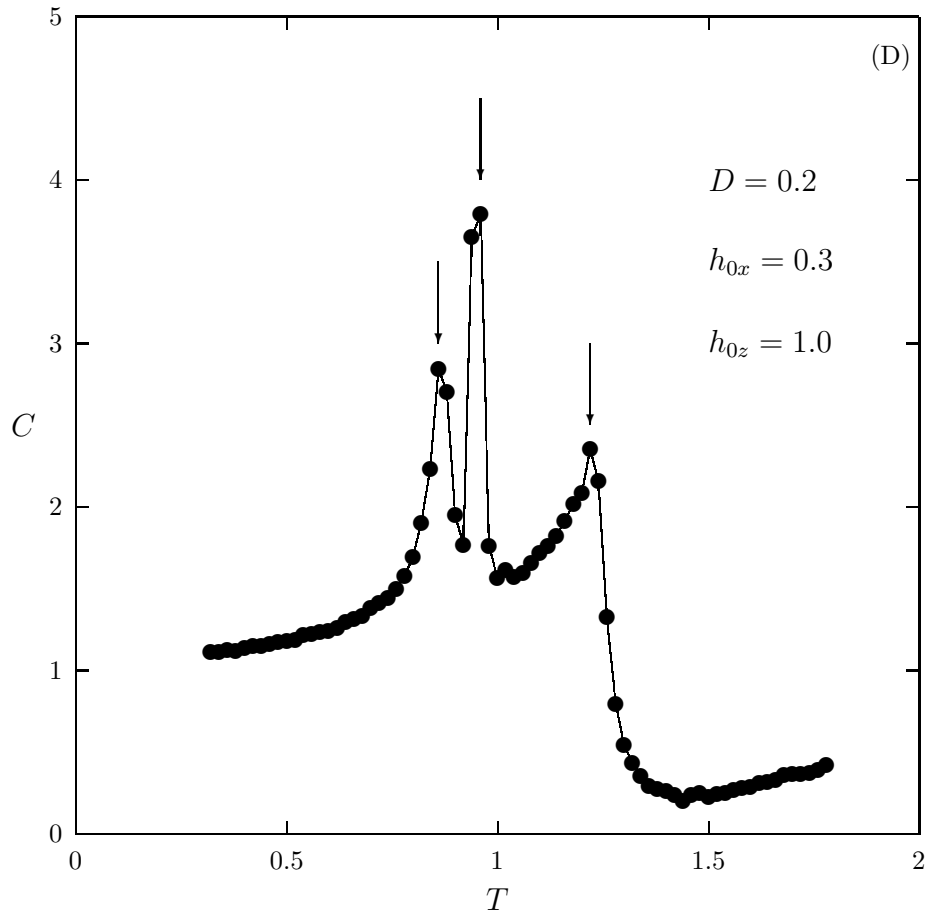


Fig.2d

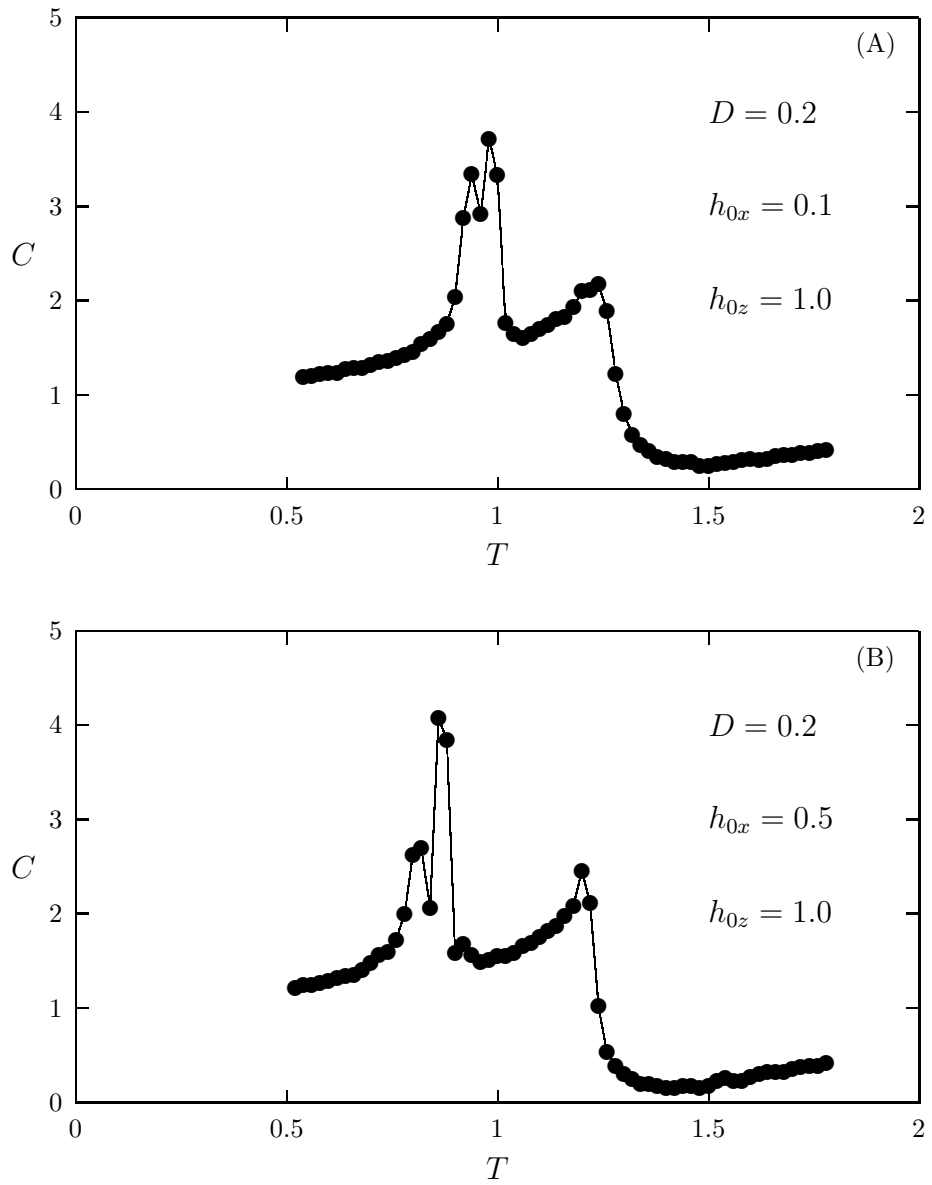


Fig.3

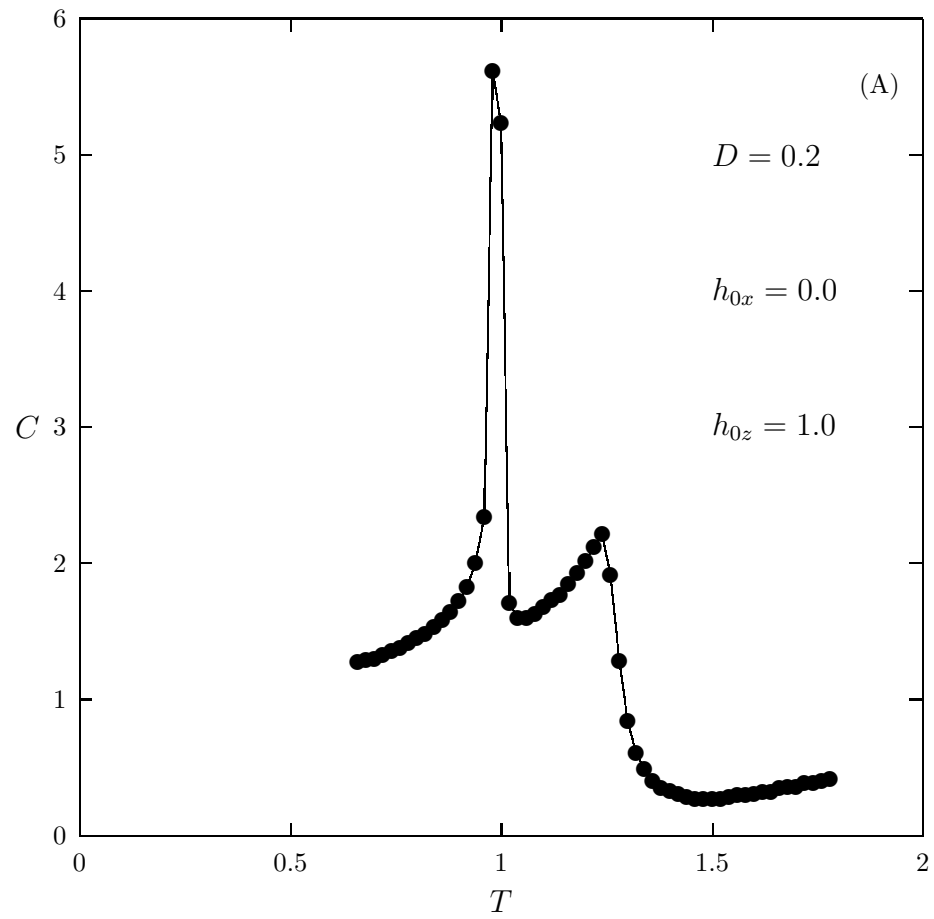


Fig.4a

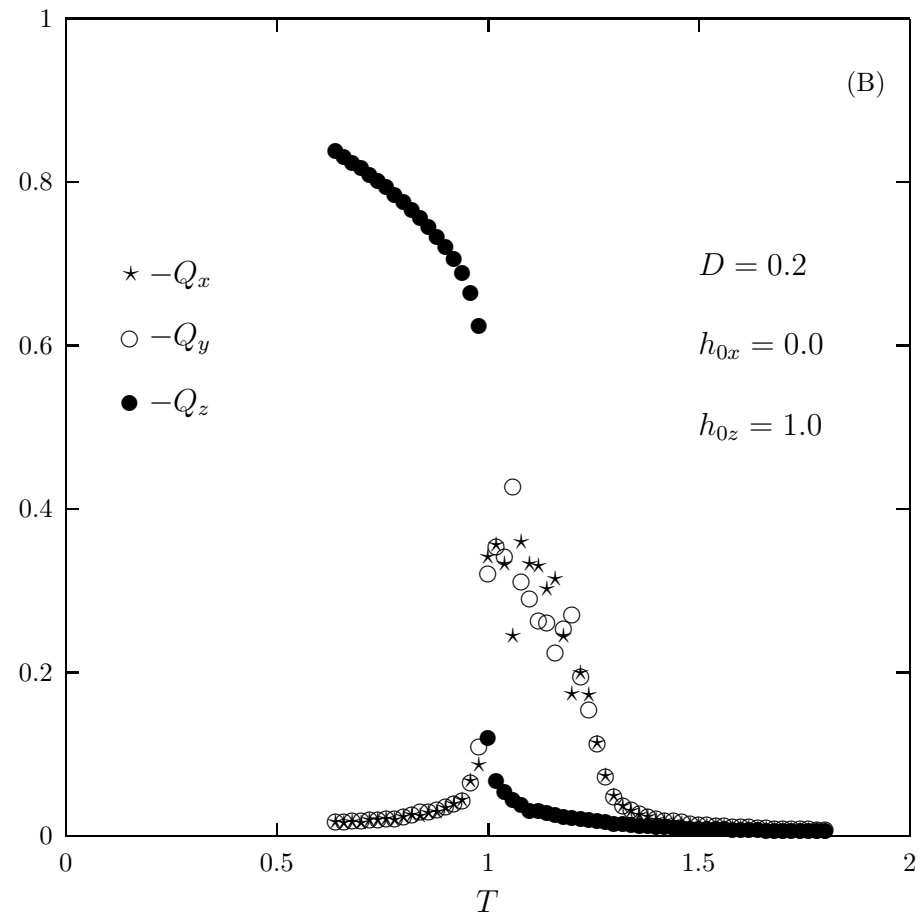


Fig.4b

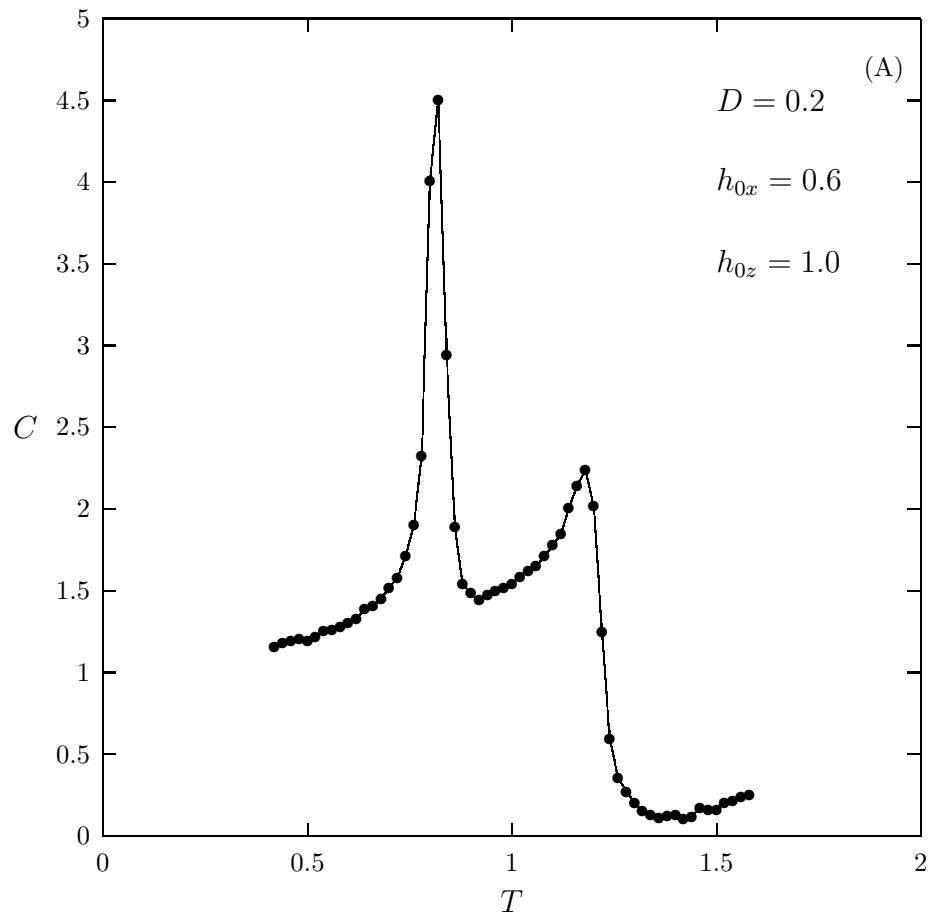


Fig.5a

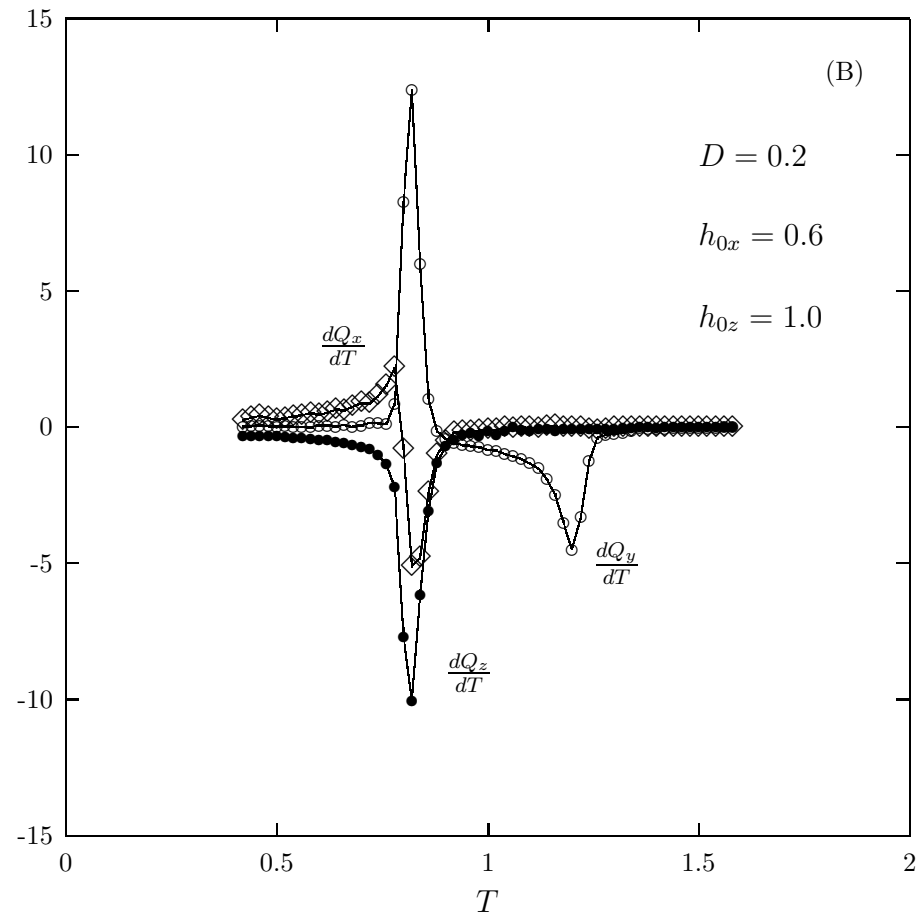


Fig.5b

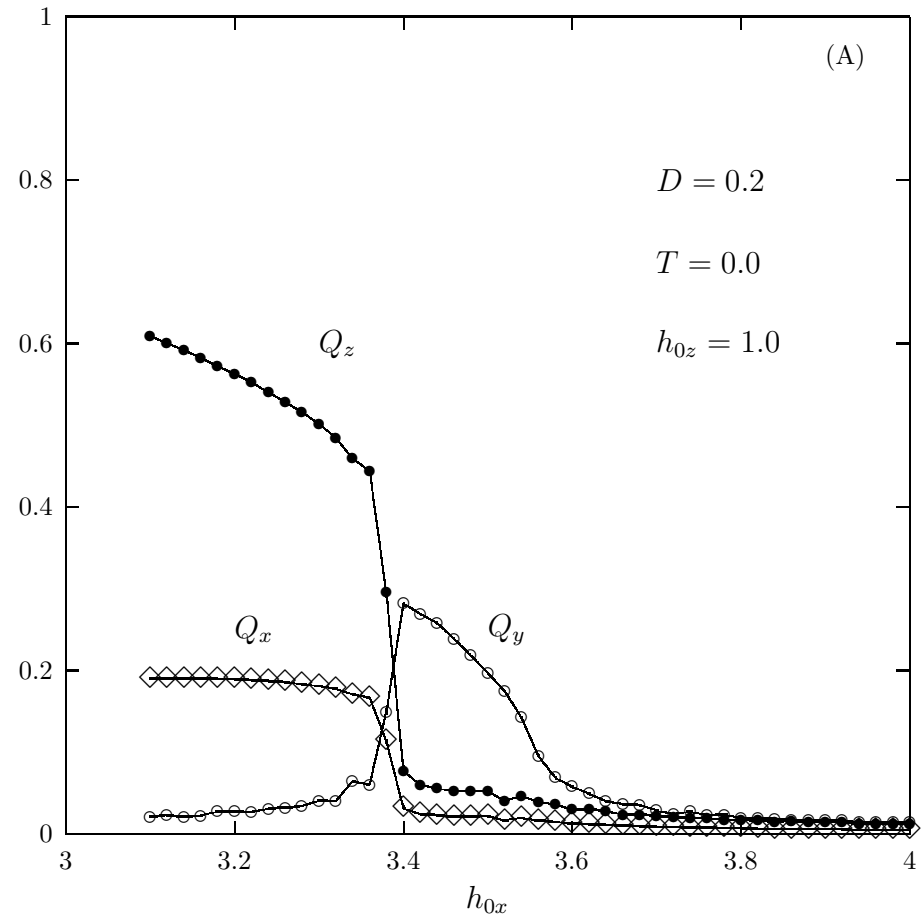


Fig.6a

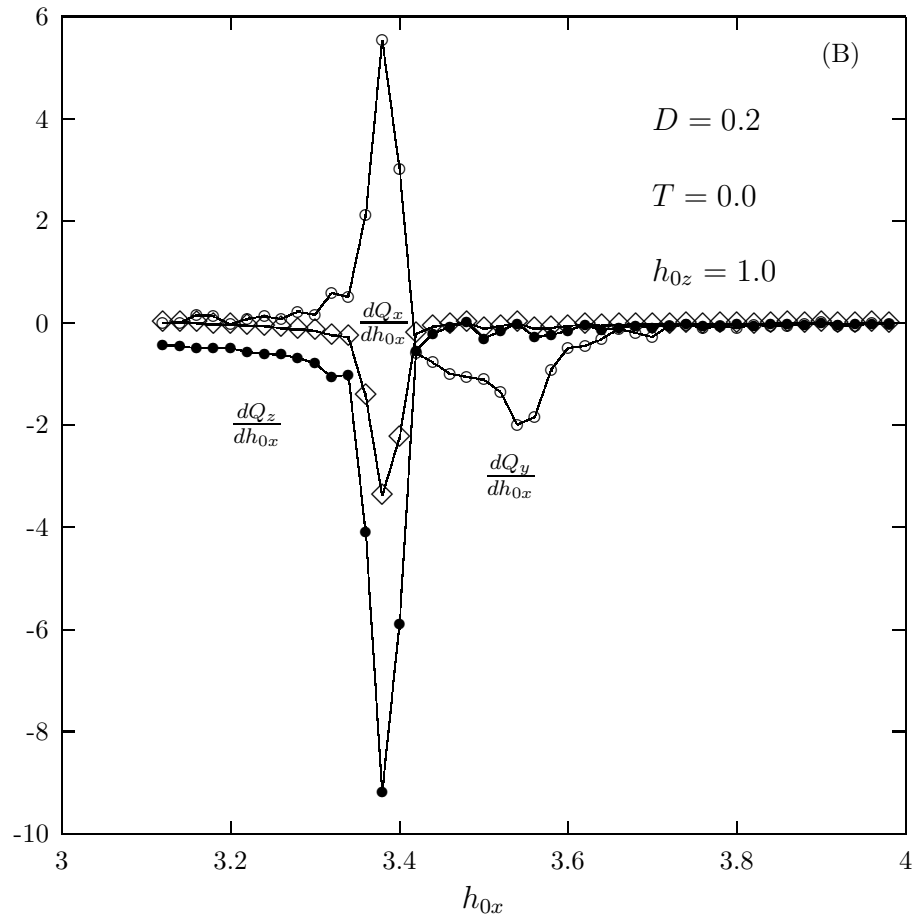


Fig.6b

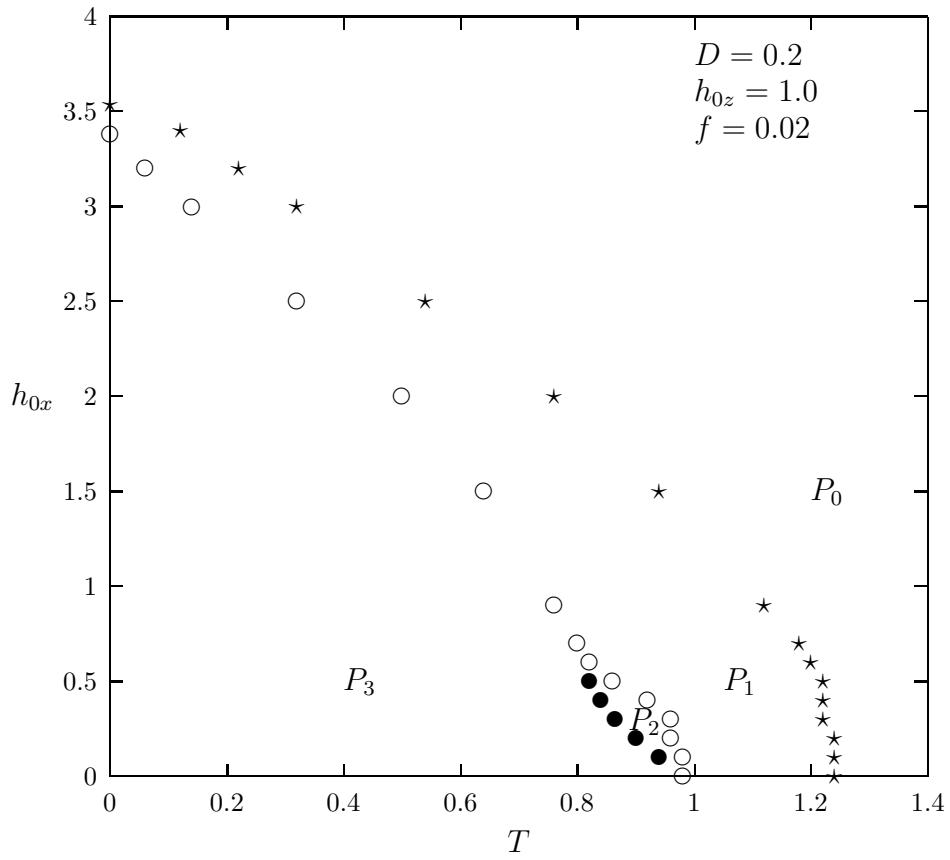


Fig.7

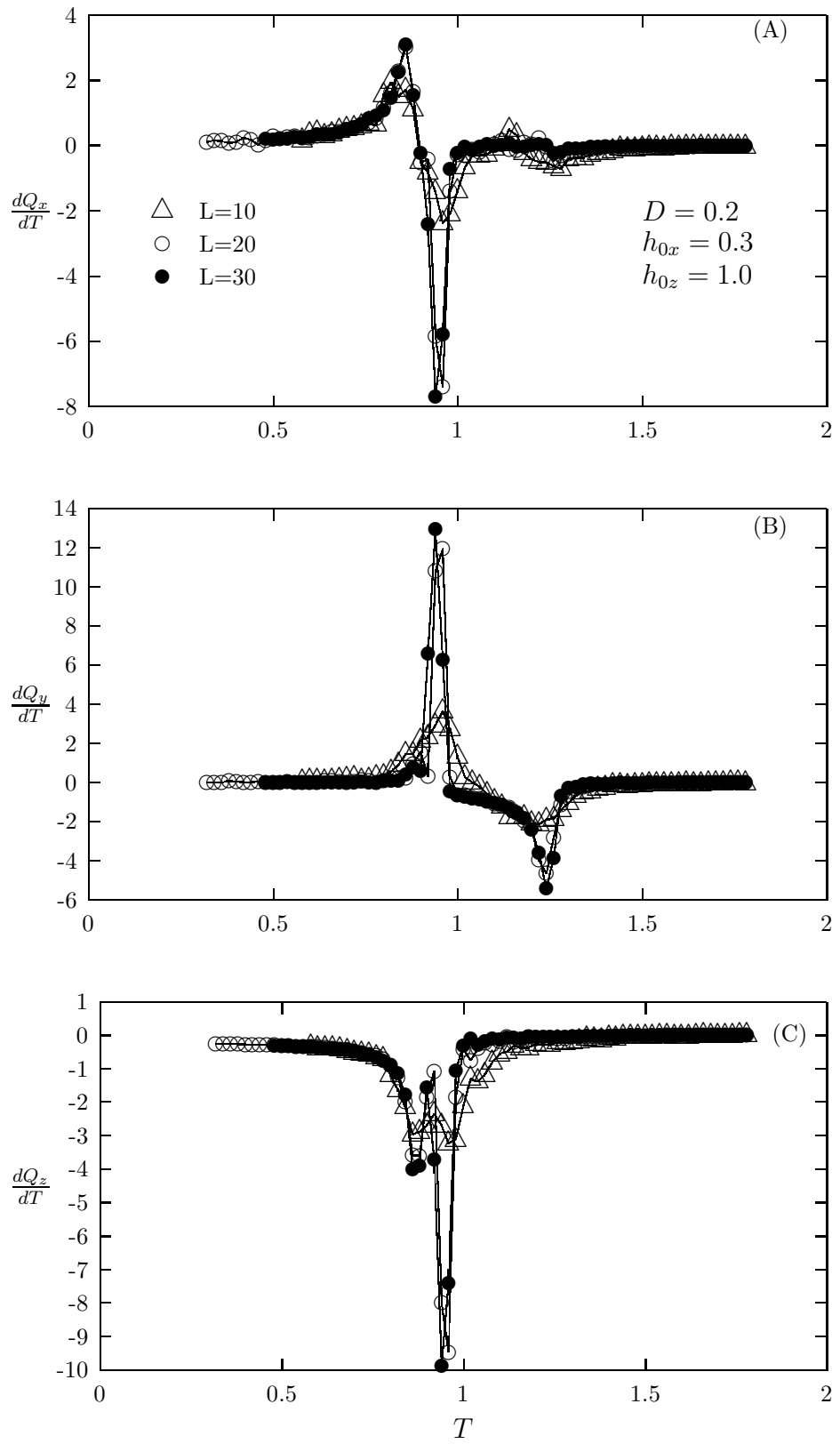


Fig.8

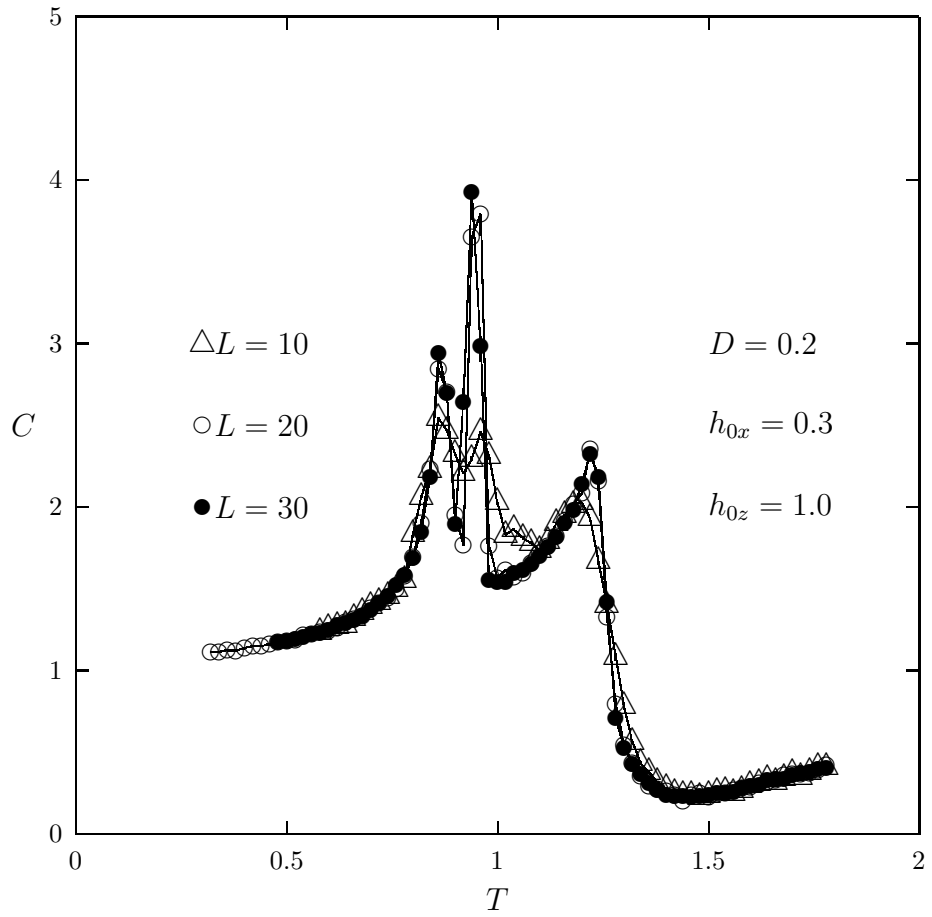


Fig.9

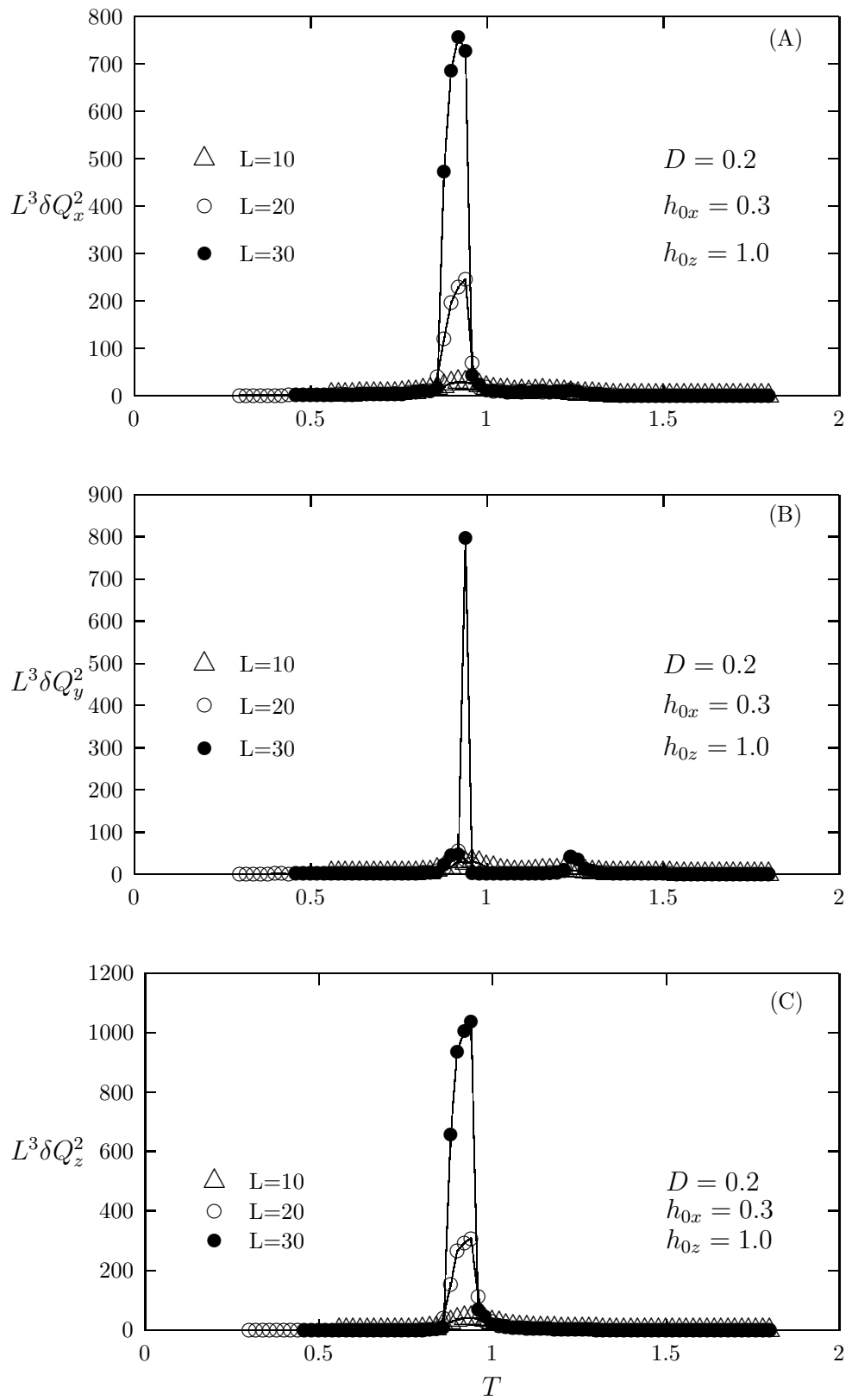


Fig.10

Heisenberg ferromagnet in polarized magnetic field: Nonequilibrium multicritical behaviour

Muktish Acharyya

Department of Physics, Krishnanagar Govt. College, PO-Krishnanagar, Dist-Nadia, PIN-741101, WB, India

E-mail: muktish@vsnl.net

The Heisenberg ferromagnet (uniaxially anisotropic along z-direction), in the presence of time dependent (but uniform over space) magnetic field, is studied by Monte Carlo simulation. The time dependent magnetic field was taken as elliptically polarized (such that the resulting field vector rotates in the XZ-plane. In the limit of low anisotropy, the dynamical responses of the system is studied as a function of temperature and the amplitudes of the magnetic field. As the temperature decreases, it was found that the system undergoes three successive dynamical phase transitions. In this limit, the multiple transitions was studied in details and the phase diagram for multicritical behavior was drawn in field amplitude and temperature plane. The transitions are supported by finite size study. The temperature variations of the variances of dynamic order parameter components (for different system sizes) indicate the existence of a diverging length scale near the dynamic transition points.

PACS numbers(s): 64.60.-i, 05.45.-a, 75.60.-d, 75.70.-i

INTRODUCTION

The nonequilibrium dynamical phase transition [1], particularly in the kinetic Ising model, has drawn immense interest of the researchers working in the field of nonequilibrium statistical physics. The dynamic transition in the kinetic Ising model in the presence of sinusoidally oscillating magnetic field was noticed [2] first in the mean field solution of the dynamical equation for the average magnetisation. Due to the absence of fluctuations, in the mean field study, the dynamic transition would be possible also even in the static (zero frequency) limit. But the true dynamic transition should never occur in the static limit due to the presence of nontrivial thermodynamic fluctuations. The occurrence of the true dynamic transitions for models, incorporating the thermodynamic fluctuations, was later shown in several Monte Carlo studies [1].

Since, the Ising model is quite simple and prototype to study the nonequilibrium dynamical phase transitions, a considerable amount of work was done on it [1]. Among these, several studies were done to establish that all these transitions have some features which are similar to well known thermodynamic phase transitions. The divergence of "time scale" [3] and the "dynamic specific heat" [3] and the divergence of "length scale" [4] are two very important observations to establish that the dynamic transition, in kinetic Ising model driven by sinusoidally oscillating magnetic field, is indeed a thermodynamic phase transition.

The dynamic phase transition in kinetic Ising model is an interesting phenomenon and act as a simple example to grasp the various features of nonequilibrium phase transitions. But it has several limitations. Since the orientations of the spins are limited by only two (up/down) directions, some interesting features of dynamic transitions (related to the dynamical transverse ordering) cannot be observed in Ising model. The classical vector spin model [5] would be the proper choice to study such interesting phenomena which are missing in Ising model. The "off-axial" dynamic transition [6] recently observed in Heisenberg ferromagnet is an example of such interesting phenomena. In the "off-axial" dynamic transition, the dynamical symmetry along the axis of anisotropy can be broken dynamically by applying an oscillating magnetic field along any perpendicular direction. There are several important studies are done on classical vector spin model driven by oscillating magnetic field. The dynamic phase transition in an anisotropic XY ferromagnet driven by oscillating magnetic field was recently studied [7] by solving Ginzburg-Landau equation. The dynamic phase transition and the dependence of its behaviour on the bilinear exchange anisotropy of classical Heisenberg ferromagnet (thin film), was studied by [8] Monte Carlo Simulation. The dynamic transitions alongwith hysteresis scaling in Heisenberg ferromagnet was also studied [9] both by Monte Carlo simulation and mean field solution.

All these studies (discussed in above paragraph) of dynamic transition in classical vector spin model gives single dynamic transition. There are few studies in Heisenberg ferromagnet where the multiple dynamic transition was reported [10, 11]. A recent study [10] of dynamical phase transition in thin Heisenberg ferromagnetic films with bilinear exchange anisotropy has shown multiple phase transitions for the surface and bulk layers of the film at different temperatures. However, another study [11] shows triple dynamic transitions (at three different temperatures) of bulk dynamic order in uniaxially anisotropic Heisenberg ferromagnet driven by elliptically polarized magnetic field. In this paper, the multiple dynamic transition (bulk only) [11] in uniaxially anisotropic Heisenberg ferromagnet driven by elliptically polarized magnetic field, is studied extensively.

In this paper, the multicritical behavior in the uniaxially anisotropic classical Heisenberg ferromagnet is studied by Monte Carlo simulation. The various dynamical phases were found. The multiple dynamic phase transition was observed by studying the temperature variation of dynamic specific heat and the derivatives of dynamic order parameter components. A finite size study was done supporting the multiple dynamic phase transitions. A length scale was found to diverge near the dynamic transition points. And finally and most importantly, the phase diagram for this multicritical behavior was drawn.

The paper is organized as follows: in the next section the description of the system, i.e., the Heisenberg ferromagnet in polarized magnetic field, is given, section III describes, the Monte Carlo simulation technique for this type of classical vector spin model, in detail. the numerical results with diagrams are reported in section IV and the paper ends with a summary in section V.

HEISENBERG FERROMAGNET IN POLARIZED MAGNETIC FIELD

The classical anisotropic (uniaxial and single-site) Heisenberg model, with nearest neighbour ferromagnetic interaction in the presence of a magnetic field can be described by the following Hamiltonian:

$$H = -J\Sigma_{\langle ij \rangle} \mathbf{S}_i \cdot \mathbf{S}_j - D\Sigma_i (S_{iz})^2 - \mathbf{h} \cdot \Sigma_i \mathbf{S}_i. \quad (1)$$

In the above expression, $\mathbf{S}_i[S_{ix}, S_{iy}, S_{iz}]$ represents a classical spin vector (situated at the i th lattice site) of magnitude unity, i.e., $|\mathbf{S}| = 1$ or $S_{ix}^2 + S_{iy}^2 + S_{iz}^2 = 1$. The classical spin vector \mathbf{S}_i may take any (unrestricted) angular orientation in the vector spin space. The first term, in the Hamiltonian,

represents the nearest -neighbour ($<ij>$) ferromagnetic ($J > 0$) interaction. The factor D , in the second term, represents the strength of uniaxial (z axis here) anisotropy which is favoring the spin vector to be aligned along the z axis. This is readily seen since the second term minimizes energy for maximization of the value of S_i^z . Here, it may be noted that for $D \rightarrow \infty$ the system goes to Ising limit and for $D = 0$ the system is in the isotropic Heisenberg limit. The last term stands for the interaction with the externally applied time dependent magnetic field $[\mathbf{h}(h_x, h_y, h_z)]$. The magnetic-field components are sinusoidally oscillating in time, i.e., $h_\alpha = h_{0\alpha} \cos \omega t$, where $h_{0\alpha}$ is the amplitude and ω is the angular frequency ($\omega = 2\pi f$; f is the frequency) of the α th component of the magnetic field. In the present study, the field is taken elliptically polarized. In general, the field vector is represented as

$$\mathbf{h} = \hat{x}h_x + \hat{y}h_y + \hat{z}h_z = \hat{x}h_{0x}\cos(\omega t) + \hat{z}h_{0z}\sin(\omega t). \quad (2)$$

The time eliminated relation between $h_x (= h_{0x}\cos(\omega t))$ and $h_z (= h_{0z}\sin(\omega t))$ is

$$\frac{h_x^2}{h_{0x}^2} + \frac{h_z^2}{h_{0z}^2} = 1. \quad (3)$$

This is the equation of an ellipse which indicates that the magnetic field vector is elliptically polarized (for $h_{0x} \neq h_{0z}$) and lies on the $X - Z$ plane. For $h_{0x} = h_{0z} = h_0$ (say), the field will be circularly polarized and $h_x^2 + h_z^2 = h_0^2$. The magnetic fields and the strength of anisotropy D are measured in the unit of J . The model is defined on a simple cubic lattice of linear size L with periodic boundary conditions applied in all three (x, y, z) directions.

MONTE CARLO SIMULATION METHOD

Monte Carlo (MC) simulation method was employed to study the above described model. The algorithm is [12] described below. The system is slowly cooled down from a random initial spin configuration [14], to obtain the steady state spin configuration at a particular temperature T (measured in the unit of J/k_B , where k_B is the Boltzmann constant). The initial random spin configuration was generated as follows [6, 14]: two different (uncorrelated) random numbers r_1 and r_2 (uniformly distributed between -1 and +1), are chosen in such a way that $R^2 = r_1^2 + r_2^2$ becomes less than or equal to unity. The set of values of r_1 and r_2 , for which $R^2 > 1$, are rejected. Now, $S_{ix} = 2ur_1$, $S_{iy} = 2ur_2$ and $S_{iz} = 1 - 2R^2$, where $u = \sqrt{1 - R^2}$. After preparing initial random configuration of spins (this is the proper spin configuration corresponding to very high temperature), one has to find steady state configuration for any fixed temperature T . For any fixed set of values of h_{0x} , h_{0z} , ω and D and at any particular temperature T , a lattice site i has been chosen randomly (random updateing scheme). The value (random direction) of the spin vector at this randomly chosen site is \mathbf{S}_i (say). The energy of the system is given by the Hamiltonian (Eq. 1). A test spin vector \mathbf{S}'_i is then chosen at any random direction (following the same algorithm described above). For this choice of \mathbf{S}'_i , at site i the energy will be $H = -J\sum_{<ij>} \mathbf{S}'_i \cdot \mathbf{S}_j - D\sum_i (S'_{iz})^2 - \mathbf{h} \cdot \sum_i \mathbf{S}'_i$. The change in energy, associated with this change in the direction of spin vector (from \mathbf{S}_i to \mathbf{S}'_i at lattice site i), is $\Delta H = H' - H$. The Monte Carlo method [12] will decide how far this change is acceptable. The probability of change (chosen here) is given by Metropolis rate [13]

$$W(\mathbf{S}_i \rightarrow \mathbf{S}'_i) = \text{Min}[1, \exp(-\frac{\Delta H}{k_B T})]. \quad (4)$$

Now, this probability will be compared with a random number R_p (say) (uniformly distributed between zero and one). If R_p does not exceed W , the move $(\mathbf{S}_i \rightarrow \mathbf{S}'_i)$ will be accepted. In this way the spin vector \mathbf{S}_i is updated. L^3 numbers of such random updates of spins, defines one Monte Carlo step per site (MCSS) and this is considered as the unit of time in this simulation. The frequency ($f = \omega/2\pi$) of time varying magnetic field is taken 0.02 and kept constant throughout the simulation. So, 50 MCSS are required to have one complete cycle of the oscillating magnetic field and hence the time period (τ) of the field becomes 50 MCSS. Any time dependent macroscopic quantity (i.e., any component of magnetisation at any instant t) is calculated as follows: Starting with an initial random spin configuration (corresponding to high temperature disordered phase), the system is allowed to become stable (dynamically) up to 5×10^4 MCSS (i.e., 1000 complete cycle of the oscillating field). The average value of various physical quantities are calculated from further 5×10^4 MCSS (i.e., averaged over another 1000 cycles). This was checked carefully that the number of MCSS mentioned above is sufficient to achieve dynamical steady state value of the measurable quantities, etc. which would clearly show the dynamic transition points within limited accuracy. But to describe the critical behaviour very precisely (i.e., to estimate critical exponent etc) a much longer run is required. The total length of the simulation becomes 10^5 MCSS. The system is slowly cooled down (T has been reduced by a small interval $\delta T = 0.02$ here) to get the values of the statistical quantities in the lower temperature phase. Here, the last spin configuration corresponding to the previous temperature is employed to act as initial configuration for the new (lower) temperature. The CPU time required for 10^5 MCSS is approximately 30 min on an Intel Pentium-III processor.

One important point may be noted here regarding the dynamics chosen in this simulational study. Since the spin components do not commute with the Heisenberg Hamiltonian, it has intrinsic quantum mechanical dynamics. Considering the intrinsic dynamics, there was a study [16] of the structure factor and transport properties in XY model. However, this paper aims to study the nonequilibrium phase transition governed by thermal fluctuations. Keeping this in mind, one should choose the dynamics that arise only due to the interaction with thermal bath. Since the objective is different, in this paper, the dynamics chosen (arise solely due to the interaction with a thermal bath) were Metropolis dynamics. The effect of intrinsic spin dynamics is therefore not considered here.

NUMERICAL RESULTS

The Monte Carlo simulations, in the present study, were done on a simple cubic lattice of linear size $L = 20$. For a fixed set of values of amplitudes (h_{0x}, h_{0z}) and frequency (f) of polarized magnetic field, strength of anisotropy (D) and temperature (T), the instantaneous magnetization components (per lattice site) were calculated as follows: $m_x(t) = \sum_i (S_i^x/L^3)$, $m_y(t) = \sum_i (S_i^y/L^3)$ and $m_z(t) = \sum_i (S_i^z/L^3)$. The dynamic order parameter is defined as the time averaged magnetization over a full cycle of the oscillating magnetic field. In this case the dynamic order parameter \mathbf{Q} is a vector (since the magnetization is vector). The components of the dynamic order parameter are calculated as $Q_x = (1/\tau) \oint m_x(t) dt$, $Q_y = (1/\tau) \oint m_y(t) dt$ and $Q_z = (1/\tau) \oint m_z(t) dt$. The time variations of magnetization components for $D = 0.2$, $h_{0x} = 0.3$ and $h_{0z} = 1.0$ are studied and shown in Fig. 1 for different temperatures T . The steady state variations of all the magnetization components are also oscillatory (in time). Depending on the values of temperature and the field amplitudes the oscillation of magnetization components is either symmetric (about zero) or asymmetric. If the variation is symmetric, the dynamic order parameter component (α component) $Q_\alpha = (1/\tau) \oint m_\alpha(t) dt$ takes the value zero and becomes nonzero for asymmetric time variation of magnetization component. In Fig. 1(a) all the magnetization components oscillates symmetrically and gives $Q_\alpha = 0$ for all

α ($=x, y, z$). This is high temperature ($T = 1.40$ here) dynamic disordered phase. This phase is denoted as P_0 : ($Q_x = 0, Q_y = 0, Q_z = 0$). As the system is cooled down to a temperature $T = 1.16$, the Fig. 1(b) shows that the time variations of $m_x(t)$ and $m_z(t)$ is symmetric but that of $m_y(t)$ is asymmetric resulting a dynamically ordered phase of first kind P_1 : ($Q_x = 0, Q_y \neq 0, Q_z = 0$). As one cool the system further to a temperature $T = 0.88$ one gets second kind of dynamically ordered phase P_2 : ($Q_x \neq 0, Q_y = 0, Q_z \neq 0$) (Fig. 1(c)). Cooling the system further towards much lower temperature a third kind of dynamically ordered phase P_3 : ($Q_x = 0, Q_y = 0, Q_z \neq 0$) was observed and a typical is shown for $T = 0.50$ in Fig. 1(d).

The signature of such successive phase transitions are also observed by studying the temperature variations of dynamic order parameter, energy, specific heat and the temperature derivatives of dynamic order parameter components. For the same set of values $D = 0.2$, $h_{0x} = 0.3$ and $h_{0z} = 1.0$ The temperature variations of various dynamic quantities are studied and shown in Fig. 2. The temperature variations of the dynamic order parameter components Q_x , Q_y and Q_z are shown in Fig. 2(a). As the system is cooled down, from a high temperature dynamically disordered ($\mathbf{Q} = \vec{0}$) phase, it was observed that first the system undergoes a transition from dynamically disordered ($\mathbf{Q} = \vec{0}$) to a dynamically Y-ordered ($Q_y \neq 0$ only) phase P_1 and the transition temperature is T_{c1} (say). It may be noted here that the resultant vector of elliptically polarized magnetic field lies in the $x - z$ plane and the dynamic ordering occurs along the y -direction only ($Q_x = 0, Q_y \neq 0, Q_z = 0$). This is clearly an off-axial transition [6]. In the case of this type of off-axial transition the dynamical symmetry (in any direction; y here) is broken by the application of the magnetic field in the perpendicular (lies in the $x - z$ plane here) direction. As the system cools down further, this phase P_1 persists over a considerable range of temperature and at a temperature T_{c2} a second transition was observed. In this phase, the system becomes dynamically ordered both in the X and Z directions at the cost of Y ordering. Usually one gets the dynamically ordered phase of second kind P_2 : ($Q_x \neq 0, Q_y = 0, Q_z \neq 0$). Here, the dynamical ordering is planar (lies on $x - z$ plane) and the dynamical ordering occurs in the same plane on which the field vector lies. This transition is not off-axial. As the temperature decreases further one ends up with a low temperature dynamically ordered phase of third kind P_3 : ($Q_x = 0, Q_y = 0, Q_z \neq 0$) via a transition occurs at temperature T_{c3} . The system continues to increase the dynamical Z ordering ($Q_z \neq 0$ only) as the temperature decreases further. The low temperature phase is only dynamically Z ordered. No further transition was observed as one cools the system further.

One gets qualitative ideas of multiple dynamic phase transitions from the above mentioned studies. However, to estimate precisely the transition temperatures T_{c1} , T_{c2} and T_{c3} further studies are required. For this reason, the temperature variations of the derivatives (with respect to temperature) of the dynamic order parameter components are studied. The derivatives were calculated numerically by using central difference formula

$$\frac{df(x)}{dy} = \frac{f(x + \delta x) - f(x - \delta x)}{2\delta x} \quad (5)$$

Fig. 2(b) shows such variations studied as a function of temperature. The derivative $\frac{dQ_y}{dT}$, shows a sharp minimum nearly at $T = T_{c1} = 1.22$. The second transition temperature T_{c2} was estimated from the position of sharp maximum of $\frac{dQ_y}{dT}$ and the corresponding sharp minima of $\frac{dQ_x}{dT}$ and $\frac{dQ_z}{dT}$. This gives $T_{c2} = 0.96$. Slightly lower temperature than T_{c2} , one observes another maximum of $\frac{dQ_x}{dT}$ and minimum of $\frac{dQ_z}{dT}$ at the same position $T = T_{c3} = 0.88$. From this study one gets the quantitative measure of the transition temperatures of multiple dynamic transition [11].

The similar values of the transition temperatures (T_{c1}, T_{c2}, T_{c3}) for the multiple dynamic transition can be estimated independently from the study of the temperature variations of dynamic energy and

specific heat. The dynamical energy (E) is defined as the time averaged value of the instantaneous energy over a full cycle of the oscillating magnetic field. From the definition, $E = (1/\tau) \oint H dt$ (H is given in Eqn. 1). The temperature variation of E is studied and shown in Fig. 2(c). This shows three inflection points at the same location of transition temperatures estimated and mentioned above. This will be very clear if one studies the derivative of the dynamic energy, namely the dynamic specific heat $C = dE/dT$ (calculated by using central difference formula 5). The temperature variation of dynamic specific heat C was studied and shown in Fig. 2(d). It indicates three peaks at three different temperatures supporting $T_{c1} = 1.22$, $T_{c2} = 0.96$ and $T_{c3} = 0.88$. Thus the estimation of transition temperatures for the multiple dynamic transition was reexamined by another independent study. The study of the temperature variation of dynamic specific heat has another importance. It independently supports that multiple transition as well as it indicates that these transitions are indeed thermodynamic phase transitions. Now one may employ the method of studying the temperature variations of derivatives of dynamic order parameter components and the dynamic specific heat to estimate the transition points. One gets three different dynamic transitions for the parameter values $D = 0.2$, $h_{0x} = 0.3$ and $h_{0z} = 1.0$. This three transitions scenario is observed for a range of values of h_{0x} (keeping other parameters fixed $D = 0.2$ and $h_{0z} = 1.0$) between $h_{0x} = 0.1$ to $h_{0x} = 0.5$ (within the precision considered here). The temperature variations of dynamic specific heat C are shown in fig 3 for two different values of h_{0x} ($= 0.1$ and 0.5). Both show the three dynamic transitions. It may be noted from fig. 3 that the transition temperature decreases as the amplitude h_{0x} increases. Now, let us see what happens if one takes the value of the x -amplitude of elliptically polarized magnetic field, i.e., h_{0x} , outside this range, keeping all other parameter values unchanged.

For $h_{0x} = 0.0$ (effectively the field is now linearly polarized along z direction only), to estimate the transition points the temperature variations of dynamic specific heat was studied and plotted in fig. 4(a). This shows two distinct and well separated peaks indicating two dynamic transitions, one at $T = 1.24$ and other at $T = 0.98$. Now to characterise the different phases the temperature variations of dynamic order parameter components were studied. This study is shown in fig. 4(b). This shows that the system gets dynamically ordered first from a high temperature disordered phase in the x and y direction. So, the high temperature *ordered phase* ($Q_x \neq 0$, $Q_y \neq 0$, $Q_z = 0$) is quite different from P_1 (described above for $h_{0x} \neq 0$). The second (low temperature ordered phase) is P_3 type. This transition (from high temperature ordered phase to low temperature ordered phase) occurs at $T_{c3} = 0.98$. So, one gets two distinct transitions for $D = 0.2$, $h_{0x} = 0.0$ and $h_{0z} = 1.0$. It may be noted here that the temperature variations of the order parameter components, mainly Q_x and Q_y , are quite scattered (near the low temperature transition). Here, Q_x and Q_y are calculated by averaging over 2000 cycles discarding first 2000 cycles ($10^5 MCSS$). For this reason the derivatives dQ_x/dT and dQ_y/dT do not give smooth variation with respect to temperature and are not shown.

Now if the value of h_{0x} is higher (say around $h_{0x} = 0.6$) with all other parameter values fixed (i.e., $D = 0.2$ and $h_{0z} = 1.0$) the triple dynamic transitions (for $h_{0x} = 0.3$) reduces to double transitions. Fig.5(a) shows the temperature variation of dynamic specific heat for $h_{0x} = 0.6$ (with $D = 0.2$ and $h_{0z} = 1.0$ fixed). It shows two distinct peaks indicating two different dynamic transitions at $T = 1.20$ and $T = 0.82$. So, in this case one gets two dynamically ordered phases, namely P_1 (higher temperature ordered phase) and P_3 (lower temperature ordered phase). The transition from P_1 phase to P_3 phase occurs at $T = 0.82$. The high temperature ordered phase P_1 transition (from dynamically disordered phase) occurs at $T = 1.20$. These two transitions were reexamined by studying the temperature variations of the derivatives of the dynamic order parameter. This was shown in fig. 5(b). From the figures it is clear that the two transitions occur at $T = 1.20$ and $T = 0.82$, for $h_{0x} = 0.6$.

From the above discussion it is quite clear that if one studies the dynamic phase transitions by

varying h_{0x} only (keeping $D = 0.2$ and $h_{0z} = 1.0$ fixed), one would get two transitions for $h_{0x} = 0.0$. Just above $h_{0x} = 0.0$, i.e., starting from $h_{0x} = 0.1$ upto $h_{0x} = 0.5$ one would get three transitions (and three ordered phases). Above this value, say $h_{0x} = 0.6$ one would get again two transitions (two ordered phases). If one continues further, it was observed that the two transitions feature continues. The transition points (temperatures) are estimated by studying specific heat and the derivatives of the dynamic order parameter components. These are not shown in figure, only the results (obtained from the peak positions of the specific heat and positions of maximum or minimum of $\frac{dQ_\alpha}{dT}$) are taken. It was observed further that all the transition points shift towards lower temperatures for higher values of h_{0x} . The whole results of this multiple transitions can be framed in $T - h_{0x}$ plane to get the multiple dynamic phase boundary. At $T = 0$ the transitions will be governed by h_{0x} only and to get complete (and closed) phase boundary one has to know the transition points for $T = 0$. The athermal dynamic transitions (for $T = 0$) were obtained from a separate zero-temperature simulational study. In this method the trial move will be accepted if it lowers the energy. Probabilistic comparison was not done here. The results for this study are shown in fig. 6. The order parameter components are studied as a function of h_{0x} (for $T = 0.0$, $D = 0.2$ and $h_{0z} = 1.0$). Fig. 6(a) shows the variations of the components of the dynamic order parameters (Q_x , Q_y and Q_z) plotted against h_{0x} . The ordered phase for higher values of h_{0x} is P_1 (i.e., $Q_y \neq 0$ only) and transition occurs at $h_{0x} = 3.54$. As the h_{0x} decreases this phase continues upto $h_{0x} = 3.38$. Just below this value a new type of phase occurs for which $Q_x \neq 0$, $Q_y = 0$ and $Q_z \neq 0$. So along this line ($T = 0$) two transitions are observed at $h_{0x} = 3.54$ and $h_{0x} = 3.38$. These values were obtained also from the maximum/minimum of the derivatives of Q_x , Q_y and Q_z with respect to h_{0x} shown in fig.6(b)). It may be noted that the athermal ($T = 0$) dynamic phase below $h_{0x} = 3.38$ is not P_3 type.

Collecting all these results of transition points, the phase diagram for the multiple dynamic transitions was plotted. This is shown in fig. 7 and is the main result of this study. The outermost boundary separates the dynamically Y -ordered phase P_1 : ($Q_x = 0, Q_y \neq 0, Q_z = 0$) from the disordered phase P_0 : ($Q_x = 0, Q_y = 0, Q_z = 0$). The transition temperature decreases as the value of the field amplitude h_{0x} increases. The region bounded by the boundaries marked by the symbols circle and bullet is second phase characterised as P_2 : ($Q_x \neq 0, Q_y = 0, Q_z \neq 0$). This region is quite small (in area) but very clear and was observed very carefully. The transition temperatures for both the boundaries (left and right) of this phase decrease as the field amplitude h_{0x} increases. The innermost (in the $T - h_{0x}$ plane) region, whose boundary is partly marked by circle (for higher values of h_{0x}) and partly marked by bullet (for lower values of h_{0x}), represents the low temperature phase characterised by P_3 : ($Q_x = 0, Q_y = 0, Q_z \neq 0$). Here also, the transition temperature decreases as the value of the field amplitude h_{0x} increases. The nature (continuous/discontinuous) of the dynamic phase transition is not quite clear from the present observations. For lower values of h_{0x} , where the three dynamic transitions occur, the nature of the transition from P_1 phase to P_2 phase, seems to be discontinuous. It may be observed from the temperature variations of the dynamic order parameter components. However, to confirm this, one should study the distribution of dynamic order parameter near the transition point and the temperature variation of its Binder cumulant [12].

The finite size study is also done to confirm that the observation is not an artifact of limited size of the system. This study was done at a particular set ($D = 0.2, h_{0x} = 0.3, h_{0z} = 1.0$) of values of the parameters. Different statistical quantities were studied as functions of temperatures for different linear sizes ($L = 10, 20, 30$ here) of the system. This particular choice of the values of D , h_{0x} and h_{0z} is meaningful in the sense that the three transitions phenomenon was observed clearly for this particular values of parameters and the most important part of the phase boundary. Figure 8 shows the temperature variations of $\frac{dQ_\alpha}{dT}$ for $L = 10, 20$ and 30 . From the figure it is clear that both the sharpness and the height (depth) of maximum (minimum) indicating the transition points increase

as the system size increase. The specific heat is also studied as a function of temperature for different L and same set of other parameter values. This is shown in fig. 9. This also indicates that the height of the peaks (indicating the transitions) increases as the system size increases. The finite size study, done here, at least may indicate that the multiple dynamic transitions mentioned above is not an artifact of finite size effect.

Lastly, the variances of the dynamic order parameter components i.e., $L^3Var(Q_\alpha) = L^3[\langle Q_\alpha^2 \rangle - \langle Q_\alpha \rangle^2] = L^3\delta Q_\alpha^2$ are studied as function of temperature and for different system sizes. Figure 10(a) shows temperature variation of $L^3Var(Q_x) = L^3[\langle Q_x^2 \rangle - \langle Q_x \rangle^2] = L^3\delta Q_x^2$ for $L = 10, 20$ and 30 . It gets sharply peaked at around $T = T_{c2} = 0.96$ (the transition temperature from P_1 phase to P_2 phase). The height of the peak increases for larger system sizes. In fig. 10(b) the $L^3Var(Q_y)$ is plotted against temperature for different system sizes. It shows two peaks. The high temperature peak (very short in height but visible in this scale) is located at $T = 1.22$. This corresponds to the transition from disordered (P_0) to first Y-ordered (P_1) phase. The low temperature peaks are positioned at around $T = 0.96$ corresponding to the transition from P_1 to P_2 . Here, also the heights of the peaks increases systematically as the system size increases. Similar things is observed for $L^3Var(Q_z)$ and shown in fig. 10(c). Here, an important thing should be noted that this study indicates that their exists a diverging length scale at the dynamic transition points [4], for the multiple dynamic transitions in this system. It should also be noted that the transition (from P_2 to P_3) temperature T_{c3} cannot be resolved from T_{c2} in the present study.

SUMMARY

The classical Heisenberg ferromagnet (uniaxially anisotropic) in presence of a time varying polarized magnetic field and in contact with a thermal bath is studied by Monte Carlo simulation using Metropolis dynamics. The magnetic field is elliptically polarized and the field vector rotates on XZ - plane. For a very weakly anisotropic (uniaxial) system and particular set of parameter values (amplitudes of field in x and z directions) if the system cools down it undergoes successive phase transitions. For a range of values of field amplitude along x-direction, three dynamic phase transitions was observed. Keeping the values of anisotropy strength and amplitude of field along z direction fixed, the phase transitions were studied for different values of the field amplitude along the x direction. In a plane formed by the temperature and the field amplitude along x direction the phase diagram for the multiple dynamic phase transition was drawn. The finite size study was done to check that the transitions are not artifacts of limited system size. The variances of dynamic order parameter components are studied as a function of temperature taking system size as parameter. This particular study indicates the exitence of a diverging length scale at the transition points.

The dynamic transition in Ising ferromagnet can be explained simply by spin reversal and nucleation [17]. The multiple dynamic transition occurs in Heisenberg ferromagnet possibly due to the coherent spin rotation [14]. To get the clear idea about it one has to study also the dynamic configurations of spins in details. The study of the relaxation dynamics of the system in the low anisotropic limit would also help to analyse few results.

The choice of the parameter values, in the present study, are obtained from various trials. In other parameter range the multiple transitions are also possible, however this particular choice gives quite distinct results of multiple dynamic transitions. To get the complete senario of multicritical behavior, one has to change the values of field amplitude along z direction also and the three dimentional (T, h_{0x}, h_{0z}) phase diagram can be obtained. But this study requires huge computational effort. Another important study is to know how the phase boundary moves as one changes the strength of the anisotropy. For infinte anisotropy the system would behave like Ising ferromagnet and for which

the phase boundary is well studied [1]. So, the natural expectation is that the phase boundaries for the multiple transitions would shrink and will collapse to a single boundary of single phase transition. The variations of dynamic phase boundaries with frequency of the applied field would also be an interesting study. Work is in progress to this direction and the results will be reported later elsewhere.

The alternative methods of studying this multiple dynamic phase transitions in anisotropic Heisenberg ferromagnet driven by polarized magnetic field are: (i) to study Landau-Lifshitz-Gilbert equation of motion [15] with Langevin dynamics, (ii) spin wave analysis of anisotropic Heisenberg ferromagnet in presence of polarised magnetic field.

ACKNOWLEDGMENTS

The library facility provided by Saha Institute of Nuclear Physics, Calcutta, India, is gratefully acknowledged.

REFERENCES

1. M. Acharyya, Int. J. Mod. Phys. C **16** (2005) (in press) and the references therein; see also B. K. Chakrabarti and M. Acharyya, Rev. Mod. Phys. **71**, 847 (1999).
2. T. Tome and M. J. de Oliveira, Phys. Rev. A **41**, 4251 (1990).
3. M. Acharyya, Phys. Rev. E **56**, 1234 (1997); **56**, 2407 (1997)
4. S. W. Sides, P. A. Rikvold and M. A. Novotny, Phys. Rev. Lett. **81**, 834 (1998)
5. D. C. Mattis, *The Theory of Magnetism I: Statics and Dynamics*, Springer Series in Solid State Sciences No. 17 (Springer- Verlag, Berlin, 1988).
6. M. Acharyya, Int. J. Mod. Phys. C **14**, 49 (2003); **12**, 709 (2001).
7. T. Yasui *et al.*, Phys. Rev. E **66**, 036123 (2002); **67**, 019901(E) (2003).
8. H. Jang, M. J. Grimson and C. K. Hall, Phys. Rev. E **68**, 046115 (2003).
9. Z. Huang, F. Zhang, Z. Chen, Y. Du, Eur. Phys. J. B, **44**, 423 (2005)
10. H. Jang, M. J. Grimson and C. K. Hall, Phys. Rev. B **67**, 094411 (2003).
11. M. Acharyya, Phys. Rev. E **69**, 027105 (2004).
12. D. Stauffer *et al.*, *Computer Simulation and Computer Algebra* (Springer-Verlag, Heidelberg, 1989); K. Binder and D. W. Heermann, *Monte Carlo Simulation in Statistical Physics*, Springer Series in Solid-State Sciences (Springer, New York, 1997); D. P. Landau and K. Binder, in *A guide to Monte Carlo Simulations in Statistical Physics* (Cambridge University Press, Cambridge, 2000), pp. 145.
13. N. Metropolis, A. W. Rosenbluth, M. N. Rosenbluth, A. H. Teller, E. Teller, J. Chem. Phys. **21**, 1087 (1953).
14. U. Nowak, in *Annual Reviews of Computational Physics*, edited by D. Stauffer (World Scientific, Singapore, 2001), Vol. 9, p. 105; D. Hinzke and U. Nowak, Phys. Rev. B **58**, 265 (1998).

15. D. Hinzke, U. Nowak and K. D. Usadel, in *Structure and Dynamics of Heterogeneous Systems*, Eds. P. Entel and D. E. Wolf (World Scientific, Singapore, 1999), pp. 331-337.
16. M. Krech and D. P. Landau, Phys. Rev. B 60, 3375 (1999)
17. M. Acharyya and D. Stauffer, Eur. Phys. J. B 5, 571 (1998)

Figure Captions

Figure 1: The time variations of the magnetisation components m_x (dot), m_y (line) and $m_z(\bullet)$ for $D = 0.2$, $h_{0x} = 0.3$ and $h_{0z} = 1.0$ and for different values of temperatures. (A) $T = 1.40$, (B) $T = 1.16$, (C) $T = 0.88$ and (D) $T = 0.40$

Figure 2: The temperature variations of different dynamical quantities for $D = 0.2$, $h_{0x} = 0.3$ and $h_{0z} = 1.0$. (A) The components of dynamic order parameter Q_x , Q_y and Q_z . The typical sizes of the error bars of Q_x , Q_y and Q_z are around 0.03 near the transition points and around 0.001 away from transition points. (B) derivatives of dynamic order parameters, (C) the dynamic energy and the (D) dynamic specific heat. Solid lines are guide to the eye. The vertical arrows in (C) and (D) indicates the transition points.

Figure 3: The temperature variations of dynamic specific heat for $D = 0.2$, $h_{0z} = 1.0$. (A) for $h_{0x} = 0.1$ and (B) for $h_{0x} = 0.5$. Solid lines are guide to the eye.

Figure 4: The temperature variations of (A) dynamic specific heat and (B) order parameter components. For $D = 0.2$, $h_{0x} = 0.0$ and $h_{0z} = 1.0$. Solid line in (A) is guide to the eye

Figure 5: The temperature variations of (A) dynamic specific heat (B) derivatives of order parameter components. For $D = 0.2$, $h_{0x} = 0.6$ and $h_{0z} = 1.0$. Solid lines are guide to the eye.

Figure 6: Athermal ($T = 0$) multiple dynamic transitions. The plots of (A) order parameter components and (B) derivatives of order parameter components with respect to h_{0x} , as functions of h_{0x} . For $T = 0$, $D = 0.2$ and $h_{0z} = 1.0$. Solid lines are guide to the eye.

Figure 7: The phase diagram in $T - h_{0x}$ plane for the multiple dynamic transitions for $D = 0.2$ $f = 0.02$ and $h_{0z} = 1.0$.

Figure 8: Temperature variations of derivatives of dynamic order parameter components for different system sizes ($L = 10, 20$ and 30) for $D = 0.2$, $h_{0x} = 0.3$ and $h_{0z} = 1.0$. (A) $\frac{dQ_x}{dT}$ versus T . (B) $\frac{dQ_y}{dT}$ versus T . (C) $\frac{dQ_z}{dT}$ versus T . Solid lines are guide to the eye.

Figure 9: Temperature variations of dynamic specific heat for different system sizes ($L = 10, 20$ and 30) for $D = 0.2$, $h_{0x} = 0.3$ and $h_{0z} = 1.0$. Solid lines are guide to the eye.

Figure 10: Temperature variations of variances of the dynamic order parameter components for different system sizes ($L = 10, 20$ and 30) for $D = 0.2$, $h_{0x} = 0.3$ and $h_{0z} = 1.0$. (A) $L^3\delta Q_x^2$ versus T . (B) $L^3\delta Q_y^2$ versus T . (C) $L^3\delta Q_z^2$ versus T . Solid lines are guide to the eye.